A Framework for Simulating Hybrid MTJ/CMOS Circuits: Atoms to System Approach

Georgios Panagopoulos
Dep. of ECE, Purdue University
gpanagop@purdue.edu

Charles Augustine
Dep. of ECE, Purdue University
caugust@purdue.edu

Kaushik Roy
Dep. of ECE, Purdue University
kaushik@purdue.edu

Abstract — **A simulation framework that can comprehend the impact of material changes at the device level to the system level design can be of great value, especially to evaluate the impact of emerging devices on various applications. To that effect, we have developed a SPICE-based hybrid MTJ/CMOS (magnetic tunnel junction) simulator, which can be used to explore new opportunities in large scale system design. In the proposed simulation framework, MTJ modeling is based on Landau-Lifshitz-Gilbert (LLG) equation, incorporating both spin-torque and external magnetic field(s). LLG along with heat diffusion equation, thermal variations, and electron transport are implemented using SPICE-inbuilt voltage dependent current sources and capacitors. The proposed simulation framework is flexible since the device dimensions such as MgO thickness and area, are user defined parameters. Furthermore, we have benchmarked this model with experiments in terms of switching current density (J_C), switching time (T_{SWITCH}) and tunneling magneto-resistance (TMR). Finally, we used our framework to simulate STT-MRAMs and magnetic flip-flops (MFF).**

Keywords-SPICE; LLG; MTJ; STT-MRAM; simulation framework

I. INTRODUCTION

Recent advances in spintronics, especially experiments showing the switching of nano-magnets with spin polarized current, has led to the possibility of very high density on-chip magnetic storage with zero leakage power, and logic styles that can potentially have very low intrinsic power consumption [1]-[3]. Most of the nano-magnetic devices use magnetic tunnel junctions (MTJs) or spin-valves [5] to efficiently write/read the magnets. However, reading/writing may require the use of simple CMOS devices. Hence, there is a need to efficiently simulate hybrid MTJ/CMOS devices and circuits to evaluate their impact on system design. Note that, such circuits use both electron "charge" and "spin" as state variables [1]. Recently, memories [2], flip-flops [4] and full adders [6] based on MTJ/CMOS technologies have also been proposed.

Even though hybrid MTJ/CMOS technologies can offer benefits at the device level, there is a need to evaluate their true potential for replacing conventional CMOS logic and memories. In addition, for any technology to become the main stream, we need a way of automating the design through conventional computer aided design (CAD) tools and flows. Thus, developing a compact SPICE framework for simulating hybrid MTJ/CMOS circuits is necessary.

Recently, various SPICE-based models have been proposed to meet the requirements mentioned above [7]-[9]. However, all of these models have their limitations. In [7] researchers have shown that using a bi-stable sub-circuit, the performance of an MTJ can be captured. To implement this model MTJ/circuit level parameters such as parallel and anti-parallel resistance (R_P, R_{AP}), and the critical switching current (I_C) along with several empirical parameters need to be provided. Hence, for simulating new MTJs, the user has to again determine new parameters to match experimental data, which can be time consuming. In addition, it cannot capture the real magnet dynamics (such as the precessional motion of electrons) which are important in predicting the failures due to process variations [10]. In [8] researchers have presented a model that is able to capture the dynamics of MTJ using analytical I-V functions for MTJs. The main drawback of this model is the absence of temperature effects on MTJs. Finally, in [9] a compact model written in C language which can be integrated with SPICE is presented. Even though this model can provide switching delay and switching power, it does not capture the effects of temperature on MTJ by solving stochastic LLG (12).

In this paper, we propose a physics-based simulation framework for hybrid MTJ/CMOS circuits implemented completely in SPICE — using only inbuilt components (capacitors, and voltage/current dependent voltage/current sources). The benefits of this model include accuracy, fast simulation time, compatibility with existing MOSFET SPICE models, ease of implementation and usability. The capability of the proposed model includes: (a) circuit analysis under process variations, such as variations of MTJ parameters (e.g. T_{ox}, MTJ area) and transistor parameters (V_{th}, W, L, T_{ox}), (b) encapsulation in the Cadence design flow, (c) application to other memory structures or hybrid MTJ/CMOS circuits, and (d) ability to be easily adapted into new MTJ process technologies (such as In-plane Magnet Anisotropy, IMA, and Perpendicular Magnet Anisotropy, PMA). By tuning the physical/material parameters at the device level, the user of this framework can predict their effects at the circuit level (e.g. power and delay).

The organization of the paper is as follows. In section II, we discuss the basic theory of MTJs and their SPICE implementation. The simulation results for MTJs are presented in section III and hybrid MTJ/CMOS circuits are presented in section IV. The conclusions are drawn in section V.

II. FRAMEWORK DESCRIPTION

A. Theory and Basic Equations

In this section, we briefly present the fundamentals of MTJs together with the basic equations which are emulated using SPICE elements. MTJ is a magnetic device and consists of two ferromagnetic layers which are separated by an oxide such as MgO or Al_2O_3. Since the size of the ferromagnets is within single-domain limits, each of them can be approximated by a mono-domain Stoner-Wohlfarth magnetic body [11] and characterized by its magnetization vector. In an

978-3-9810801-8-6/DATE12/©2012 EDAA

MTJ structure one ferromagnet has fixed magnetization vector (fixed layer) while the magnetization vector of the other is free to move (free layer). The relative position of these two magnetization vectors, which is designated as $\vec{\boldsymbol{M}}(t)$, determine the MTJ resistance. Since one of these layers is fixed, we can assign $\vec{\boldsymbol{M}}(t)$ as the magnetization vector of the free layer. Moreover, $\vec{\boldsymbol{M}}$ is assumed to be constant in magnitude, and hence its dynamics can be represented by the corresponding normalized unit vector $\vec{\boldsymbol{m}}(t) = \vec{\boldsymbol{M}}/M_S$, where M_S is the ferromagnet's saturation magnetization. Physically, the motion of $\vec{\boldsymbol{m}}(t)$ is dictated by the torques it experiences due to uniaxial anisotropy field ($\vec{\boldsymbol{T_U}}$), easy-plane anisotropy field ($\vec{\boldsymbol{T_K}}$), external magnetic field ($\vec{\boldsymbol{T_H}}$) and spin torque ($\vec{\boldsymbol{T_S}}$). The dynamics of $\vec{\boldsymbol{m}}(t)$ is predicted by the Landau-Lifshitz-Gilbert (LLG) nonlinear differential equation [11]:

$$\frac{d\vec{\boldsymbol{m}}(t)}{dt} + \alpha\left(\vec{\boldsymbol{m}}(t) \times \frac{d\vec{\boldsymbol{m}}(t)}{dt}\right) = \gamma\vec{\boldsymbol{T}} \quad (1)$$

where $\vec{\boldsymbol{T}} = \vec{\boldsymbol{T_U}} + \vec{\boldsymbol{T_K}} + \vec{\boldsymbol{T_H}} + \vec{\boldsymbol{T_S}}$, α is the LLG damping coefficient and γ is the gyromagnetic ratio. Since the magnitude of $\vec{\boldsymbol{m}}(t)$ is 1, we converted (1) into the spherical coordinate system where the position of the vector in 3-D space is specified uniquely by the angles θ and φ. Eq. (1) can be written in spherical coordinates as:

$$\frac{1+\alpha^2}{\gamma H_k}\begin{bmatrix}\dot{\theta}\\ \dot{\varphi}\end{bmatrix} = \vec{\boldsymbol{T_U}} + \vec{\boldsymbol{T_K}} + \vec{\boldsymbol{T_H}} + \vec{\boldsymbol{T_S}} \quad (2)$$

where each torque component depends on θ and φ; and they are given by the following equations [11]:

$$\vec{\boldsymbol{T_U}} = -\begin{bmatrix}\alpha sin\theta cos\theta\\ cos\theta\end{bmatrix},\ \vec{\boldsymbol{T_K}} = -\boldsymbol{h_p}\begin{bmatrix}(sin\varphi + \alpha cos\theta cos\varphi)sin\theta cos\varphi\\ (cos\varphi cos\theta - \alpha sin\varphi)cos\varphi\end{bmatrix} \quad (3)$$

$$\vec{\boldsymbol{T_H}} = -\boldsymbol{h}\begin{bmatrix}cos\varphi sin\psi + \alpha(sin\theta cos\psi - cos\theta sin\varphi sin\psi)\\ \frac{(sin\theta cos\psi - cos\theta sin\varphi sin\psi - \alpha cos\varphi sin\psi)}{sin\theta}\end{bmatrix},\ \vec{\boldsymbol{T_S}} = \boldsymbol{h_s}\begin{bmatrix}-sin\theta\\ +\alpha\end{bmatrix}$$

where ψ is the angle of the external magnetic field with respect to easy axis. $\boldsymbol{h_p} = 4\pi M_S/H_k$, $\boldsymbol{h} = H/H_k$, and $\boldsymbol{h_s} = (\hbar/2q)\eta J/T_m M_s H_k$. Also, H is the magnitude of the external magnetic field, H_k is the uniaxial anisotropy field, J is the tunneling current, η is the spin polarization factor of J and T_m is the thickness of the free layer. The solutions of LLG equation are the transient trajectories of the magnetization vector $\vec{\boldsymbol{m}}$ of the free layer (see next section).

As mentioned before, θ and φ affects the tunneling resistance of MTJ. Since, spin-torque component ($\vec{\boldsymbol{T_S}}$) is generated using current flowing through MTJ, the resistance is a function of voltage (V) applied across the MTJ. In addition, the temperature also affects the electrical characteristics of MTJ [16]. Hence, MTJ tunneling resistance is a function of θ, φ, V and temperature (T) and is given by [20]:

$$R(\theta, V, T) = \frac{\sin(cT)}{cT}\cdot[\mathrm{P}_3\theta^3 + \mathrm{P}_2\theta^2 + \mathrm{P}_1\theta + R_P]\cdot(1 - \mathrm{abs}(V)/Slope)\cdot 10^{s\cdot(T_{ox} - T_{ox,0})} \quad (4)$$

where T_{ox} is the oxide thickness, R_P is the tunneling resistance in the parallel mode, V is the applied voltage, c is a material dependent parameter and *Slope* determines the voltage dependence of R_{AP}. Thus, MTJ resistance in turn determines the current flowing through the MTJ and hence, the spin-torque generated in the magnet. Heat diffusion for solving temperature in MTJ is given by:

$$C_V\rho\frac{\partial T(t,x)}{\partial t} = K\frac{\partial^2 T(t,x)}{\partial x^2} + RA_{MTJ}J_{\mathrm{MTJ}}^2\delta(x) \quad (5)$$

where T is the temperature, C_V is the heat capacitance, ρ the volume density of the material, K is the thermal conductivity,

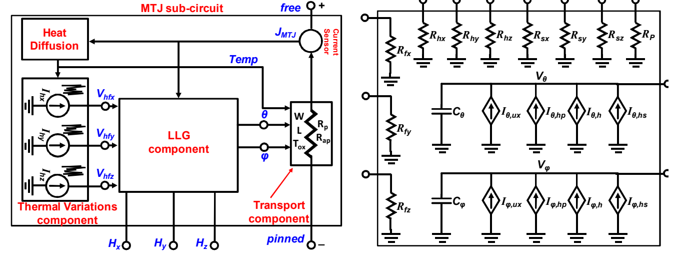

Fig. 1: Proposed MTJ SPICE sub-circuit. The arrows in the nets show the information flow. LLG SPICE component.

RA_{MTJ} is the resistance-area product of the MTJ and J_{MTJ} is the current density that flows through it. As a result, (2), (4) and (5) need to be solved self-consistently for accurate estimation of MTJ dynamics. In the next subsection, we show the implementation of our simulation framework using inbuilt SPICE elements.

B. SPICE Implementation

The proposed SPICE-based MTJ model (see Fig. 1a) consists of four components: (a) transport, (b) LLG, (c) thermal fluctuations and (d) heat diffusion. Each component is implemented using capacitors, variable resistances and current sources which are inbuilt SPICE elements. Sub-circuits for each component are presented in the next subsections.

i) Transport

Transport, emulates the time-dependent MTJ resistance which is a function of θ, φ, V and T. The physical size of MTJ free layer (W: width, L: length and T_{m}: thickness) has been incorporated as SPICE parameters.

ii) LLG

The electric circuit that emulates the system represented by (2) and (3), consists of a pair of linear capacitors with voltage dependent current sources connected in parallel as shown in Fig. 1b. The dynamic behavior of such a circuit is described by (1st Kirchhoff's law): $C\frac{dv_C}{dt} = \sum_i I_i$ (6) where v_C is the voltage across the capacitor, C is the capacitance and I_i the values of the *i*-th current source. We can exploit the similarity between (2) and (6). Thus, if we set: $C_\theta = C_\varphi = (1+\alpha^2)/\gamma H_k$ and each current source equal to the torques defined by (3), then we have a SPICE model for the LLG equation. Consequently, the circuit shown in Fig. 1b can emulate the dynamics of a magnet (that is, the free layer of MTJ in our case). Note that magnet's characteristic physical parameters (M_{s}, K_{u}, η, α) can also be incorporated as parameters in the SPICE sub-circuit. Other quantities introduced in section IIA are time dependent (i.e. $\boldsymbol{h}_{\mathrm{p}}$, $\boldsymbol{h}$, $\boldsymbol{h}_{\mathrm{s}}$) and their values are generated as voltages across a resistance as shown in Fig. 1b. Moreover, the initial voltages

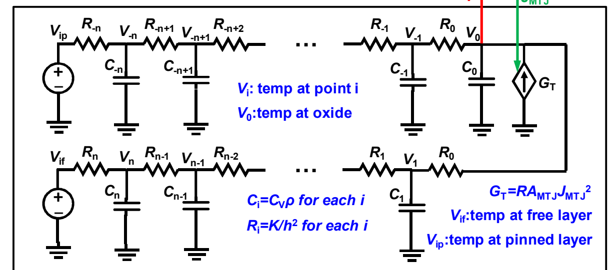

Fig. 2: Heat diffusion SPICE component.

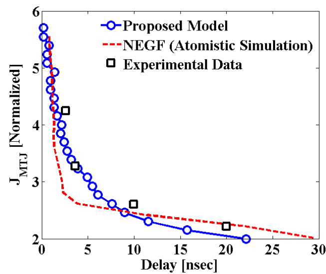

Fig. 3: Comparison of switching current density (J_{MTJ}) as a function of switching time by proposed model, NEGF [3] and experimental data [14].

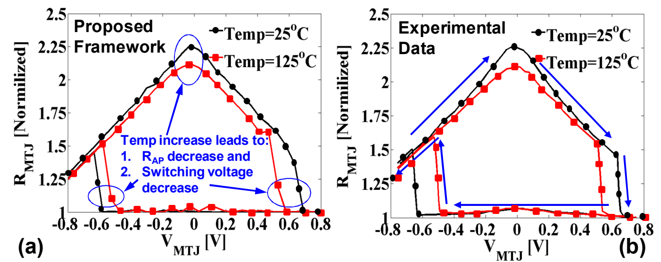

Fig. 4: The effect of temperature on MTJ switching characteristics (a) using the proposed framework and (b) comparison with experimental data [15], after model calibration.

across C_θ and C_φ specify the initial position of magnetization vector, $\vec{\boldsymbol{m}}(t)$.

iii) Thermal Variations and Temperature Effects

The effects of temperature on MTJ's behavior can be captured by using the stochastic LLG equation (SLLG) [12]. SLLG equation differs from ordinary LLG by the temperature dependent fluctuating term/torque $\vec{\boldsymbol{H_f}}$. Hence, the total torque is defined as $\vec{\boldsymbol{T_U}}+\vec{\boldsymbol{T_K}}+\vec{\boldsymbol{T_H}}+\vec{\boldsymbol{T_S}}+\vec{\boldsymbol{H_f}}$, where $\vec{\boldsymbol{H_f}}=[\boldsymbol{H_{fx}},\boldsymbol{H_{fy}},\boldsymbol{H_{fz}}]$. The mean and standard deviation of each fluctuating term are required [12]. We set the mean value of these stochastic processes to zero ensuring that SLLG will provide the same solutions as (2) over time on average. Under the assumption that the position of the magnetization vector follows Boltzmann distribution in thermal equilibrium, standard deviation of the fluctuating terms can be calculated by the following expression [12] $\sigma=\sqrt{a/(1+a)2kT/(\gamma\mu_0 M_S V)}$, where T is the temperature, k is Boltzmann's constant and $V=WLT_m$ is the volume of free layer. In SLLG the temperature is provided by solving the heat diffusion equation (5) which is discretized only in space. The corresponding SPICE component is depicted in Fig. 2. The voltage sources V_{ip} and V_{if} determine the boundary conditions, which are the temperatures at the terminals of MTJ. We set the value of these sources equal to the ambient temperature.

iv) Self-Consistent solutions

The interconnected blocks as shown in Fig. 1a, lead to self-consistent solutions of (2), (4) and (5). After benchmarking and calibration of the proposed model in section III, we present simulation results for MTJ devices and hybrid MTJ/CMOS circuits.

III. MTJ Model Calibration and Device Level Simulations

We have benchmarked our model with two separate experiments [14], [15]. In the first experiment (Fig. 3), with fixed MTJ parameters, the critical current (J_C) is varied and the corresponding switching time is captured. The proposed model can match both experimental data from [14] and Non-Equilibrium Greens Function simulation results from [2]. This shows that our framework is accurate in capturing MTJ dynamics (switching).

In the second experiment, we show the effect of temperature in MTJ resistance. In Fig. 4(a), the curve with the squares is generated for 300°K and the one with the circles for 400°K. Note that the effect of temperature on resistance is two-fold. First, increased temperature results in decreased anti-parallel resistance while the parallel resistance remains unchanged as shown in section II. Second, the critical switching current (J_C) decreases at elevated temperature because at higher temperature the effective torque due to thermal fluctuations is higher, assisting the MTJ to switch. These conclusions have also been observed experimentally in [15] and are plotted in Fig. 7(b) for comparison.

In Fig. 4, we illustrate the switching behavior of MTJ for applied voltages of 0.5V and 0.8V. Specifically, Fig. 4(a) shows the switching current and Fig. 4(b) captures the MTJ temperature. Note that in this simulation SLLG and heat diffusion are solved self-consistently. We also observe that higher applied voltage results in larger current, higher temperatures and faster switching.

IV. Applications at the Circuit Level

In this section, we present hybrid MTJ/CMOS (TSMC 65nm) circuits showing that the proposed framework can be used to simulate not only MTJ devices but also complex hybrid circuits. We consider STT-MRAM and MFF as examples.

A. STT-MRAM

STT-MRAM consists of one MTJ and one NMOS access transistor [13]. Bit-cell information is stored in the free magnetic layer of the MTJ. In the parallel case, the resistance is low (R_L) and in the anti-parallel case the resistance is high (R_H). This difference in resistance can be used to sense the data stored inside the MTJ, converting the information from magnetic to electric form. The measure of the resistance difference, called tunneling magneto-resistance (TMR), is defined as: TMR=(R_H-R_L)100/R_L. Moreover, the magnet is a non-volatile device and as a result information stored in the MTJ is non-volatile.

As we discussed in section II, there are two approaches to switch the MTJ: (a) external magnetic field (H_{ext}) and (b) current induced spin-torque. It has been shown that spin-

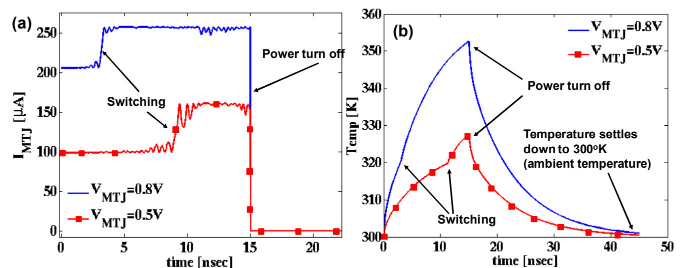

Fig. 5: The effect of temperature on MTJ dynamics: (a) MTJ current, (b) oxide temperature, (c) z-component of magnetization vector and (d) thermal variations solving SLLG. Ambient temperature is 300K. Note that both temperature and thermal variations change with time.

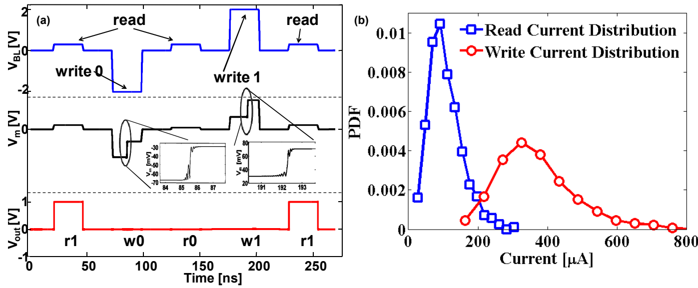

Fig. 6: (a) STT-MRAM sequence of read and write operations. Oscillations during switching are also predicted by our framework. (b) Simulation of 10000 STT-MRAM samples under process variations, i.e. Vth of NMOS, T_{ox} and area of MTJ using the proposed framework to predict the read and write distributions.

torque is a more scalable approach and hence will lead to lower power memory switching for identical stability [2]. The read and write operation in STT-MRAM and the corresponding voltages are indicated in Fig. 6a. It is important to underline the variations of the output (V_m) that occur during switching. These variations which are predicted by the proposed model validate the accuracy, not only in the switching delay but also in the true nature of the output node during switching. In STT-MRAM both read and write operations senses the current passing thought MTJ which can switch MTJ if this current exceed the critical current (I_C) [10]. In addition to the read failure, STT-MRAM also suffers from probable write failure [13]. Write failure occurs if the MTJ cannot be switched within a given write time (T_{WR}) due to insufficient current ($I<I_C$). MTJ process variations are due to MgO thickness variations, MTJ area variation and transistor variations can be lumped into threshold (V_{th}) variations. In Fig. 6b, we plot the read and the write current distribution of a sample set of 10000 STT-MRAM cells, where variations due in NMOS and MTJ parameters are considered.

B. MFF

MFF was proposed in [5] in order to reduce the standby power in Flip Flops. This circuit consists of two MTJ devices and thirty seven MOSFETs [5]. Note that this is based on the master-slave architecture and its structure is similar to 6T-SRAM cell with two additional MTJs connected in the source of the NMOS transistors. The pair of MTJs stores data bit and its complement. The data stored in the MTJs can be retained even after the power is turned off.

Transient simulation of successive reads and writes of MFF are shown in Fig. 7. Initially we turn on the power supply to restore the internal node voltages, using the stored information inside MTJs. Next, opposite data is written with the application of appropriate magnetic field generated by NOR gates [5]. We are able to match the experimentally reported MFF read and write results using the proposed model, which further increases our confidence in the model.

V. CONCLUSIONS

In this paper we have presented a SPICE-based framework to simulate hybrid MTJ/CMOS circuits. The proposed framework bridges the gap between material, devices and circuits since it provides the ability to explore performance tuning knobs at various levels of abstraction, starting from

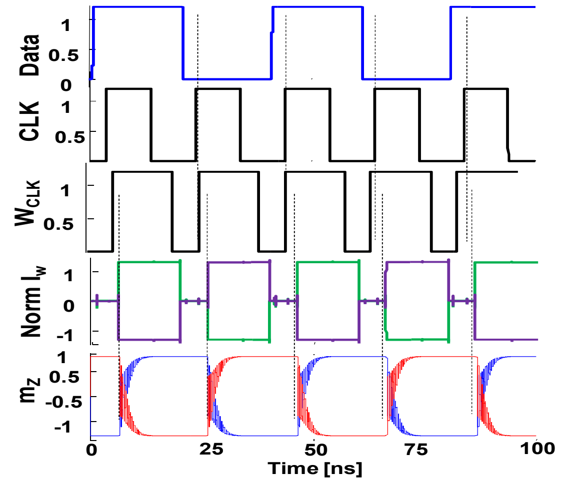

Fig. 7: MFF operation with Ku=2.6x10^{5}emu/cm^3.

materials to the circuit level. We have benchmarked this model with experimental data.

ACKNOWLEDGMENT

The authors would like to thank Dr. Arijit Raychowdhury for useful and fruitful discussions. This research was funded in part by Nano Research Initiative, INDEX center, Qualcomm, and Intel Corporation.

REFERENCES

[1] Wolf, S.A et. al, "The Promise of Nanomagnetics and Spintronics for Future Logic and Universal Memory", Proc. of IEEE, Dec. 2010.

[2] C. Augustine, et. al, "Numerical Analysis of Typical STT-MTJ Stacks for 1T-1R Memory Arrays", IEEE IEDM , pp. 544-547, December, 2010.

[3] C. Augustine, et. al, "Low-Power Functionality Enhanced Computation Architecture Using Spin-Based Devices", IEEE NANOARCH, Jun., 2011

[4] M. N. Baibich, et. al "Giant Magnetoresistance of (001)Fe/(001)Cr Magnetic Superlattices". PRLetters, pp. 2472–2475, Nov. 1988.

[5] N. Sakimura, T. Sugibayashi, R. Nebashi and N. Kasai, "Nonvolatile Magnetic Flip-Flop for standby-power-free SoCs," IEEE CICC, 2008.

[6] S. Matsunaga, et. al, "Fabrication of a Nonvolatile Full Adder Based on Logic-in-Memory Architecture Using Magnetic Tunnel Junctions", 2008.

[7] J. D. Harms, et. al., "SPICE Macromodel of Spin-Torque-Transfer-Operated Magnetic Tunnel Junctions", IEEE T-ED, June 2010.

[8] A. Nigam, et. al., "Self consistent Parameterized Physical MTJ Compact Model for STT-RAM," pp. 423–426, 2010.

[9] W. Guo, et. al., "SPICE modelling of magnetic tunnel junctions written by spin-transfer torque," JAP, 43, 2010.

[10] J. Li et. al., "Modeling of Failure Probability and Statistical Design of Spin-Torque Transfer Magnetic Random Access Memory (STT MRAM) Array for Yield Enhancement", IEEE DAC, 2008.

[11] J.Z. Sun, "Spin-current interaction with a monodomain magnetic body: A model study", PRB, Jul. 2000.

[12] W. F. Brown, "Thermal fluctuations of a single-domain particle", Phys. Rev., vol. 130, no. 5, pp. 1677-1686, June, 1963.

[13] J. Li, et. al., "Design paradigm for robust spin-torque transfer magnetic RAM from circuit/architecture perspective," IEEE TVLSI, Dec., 2010.

[14] Z. Diao, et. al, "Spin-transfer torque switching in magnetic tunnel junctions and spintransfer torque random access memory," JPCM, 2007.

[15] K. Lee and S Kang, "Design Consideration of Magnetic Tunnel Junctions for Reliable high-Temperature Operation of STT-MRAM", IEEE TMAG, Jun, 2010.

[16] L.Yan,S.Liou, D. Wang,"Temperature dependence of magnetoresistance in magnetic tunnel junctions with different free layer structures",PRB,2006.